Pneumocystis Mediates Overexpression of Antizyme Inhibitor Resulting in Increased Polyamine Levels and Apoptosis in Alveolar Macrophages[*]

Chung-Ping Liao[‡], **Mark E. Lasbury**[‡], **Shao-Hung Wang**[‡1], **Chen Zhang**[‡], **Pamela J. Durant**[‡], **Yasuko Murakami**[§], **Senya Matsufuji**[¶], and **Chao-Hung Lee**[‡2]

From the [‡]*Department of Pathology and Laboratory Medicine, Indiana University School of Medicine, Indianapolis, Indiana 46202, the* [§]*Department of Genetics & Molecular Biology, School of Pharmacy, Musashino University, Nishi-Tokyo 202-8585, Japan, and the* [¶]*Department of Molecular Biology, The Jikei University School of Medicine, Tokyo 105-8461, Japan*

Pneumocystis **pneumonia (PcP) is the most common opportunistic disease in immunocompromised patients. Alveolar macrophages are responsible for the clearance of** ***Pneumocystis*** **organisms; however, they undergo a high rate of apoptosis during PcP due to increased intracellular polyamine levels. In this study, the sources of polyamines and mechanisms of polyamine increase and polyamine-induced apoptosis were investigated. The level of ornithine decarboxylase (ODC) was elevated in alveolar macrophages, and the number of alveolar macrophages that took up exogenous polyamines was increased 20-fold during PcP. Monocytes, B lymphocytes, and CD8+ T lymphocytes that were recruited into the lung during PcP expressed high levels of ornithine decarboxylase, suggesting that these cells are sources of polyamines. Both protein and mRNA levels of antizyme inhibitor (AZI) were increased in alveolar macrophages during PcP. This AZI overexpression correlated with increased polyamine uptake by alveolar macrophages, because AZI expression knockdown decreased the polyamine uptake ability of these cells. AZI expression knockdown also decreased the apoptosis rate of alveolar macrophages.** ***Pneumocystis*** **organisms and zymosan A were found to induce AZI overexpression in alveolar macrophages, suggesting that** **β-glucan, which is the major component of the** ***Pneumocystis*** **cell wall, induces AZI overexpression. The levels of mRNA, protein, and activity of polyamine oxidase were increased in alveolar macrophages during PcP, indicating that the H_2O_2 generated during polyamine catabolism caused alveolar macrophages to undergo apoptosis. Taken together, results of this study indicate that** ***Pneumocystis*** **organisms induce AZI overexpression in alveolar macrophages, leading to increased polyamine synthesis and uptake and apoptosis rate of these cells.**

Pneumocystis is an opportunistic pathogen; it causes *Pneumocystis* pneumonia (PcP)[3] in immunocompromised individuals, especially in patients with AIDS. Advanced PcP is characterized by infiltration of inflammatory cells in the lung, thickened alveolar septa, and foamy exudates that fill the alveoli. Although host inflammatory responses are important in the defense against *Pneumocystis* infection, they may also cause lung injury leading to impaired gas exchange and respiratory failure. CD4+ T lymphocytes are crucial in the defense against *Pneumocystis* infection, because a severe decrease in the number of CD4+ T lymphocytes predisposes patients to the infection (1). Therefore, prophylaxis with a combination of trimethoprim and sulfamethoxazole (TMP-SMX) is usually given to patients with fewer than 200 CD4+ T lymphocytes per microliter in the blood. TMP-SMX interrupts folate syntheses in *Pneumocystis* organisms and is also the most common regimen for treatment of PcP. Unfortunately, TMP-SMX-resistant *Pneumocystis* organisms have emerged due to mutations in the dihydropteroate synthase gene (2–4), and some PcP patients may fail TMP-SMX therapy (3).

The alveolar macrophage is the major cell type responsible for the clearance of *Pneumocystis* organisms (5). Several macrophage receptors are involved in recognition of the organism. Mannose receptor and Dectin-1 have been shown to mediate phagocytosis of *Pneumocystis* organisms (6, 7), whereas the interaction between TLR2 and *Pneumocystis* triggers NF-κB activation, leading to increased production of TNF-α and MIP-2 (8). However, the number of alveolar macrophages is decreased during PcP in humans (9) and animals (10, 11). This defect is at least partly due to increased rate of apoptosis of alveolar macrophages during PcP (11–13). We have found that the levels of polyamines, including spermidine, N^1-acetylsper-

[1] Current address: Institute of Microbiology and Immunology, National Yang-Ming University, Taipei 112, Taiwan.
[2] To whom correspondence should be addressed: Dept. of Pathology and Laboratory Medicine, Indiana University School of Medicine, 1120 South Dr., FH419, Indianapolis, IN 46202. Tel.: 317-274-2596; Fax: 317-278-0643; E-mail: chlee@iupui.edu.

[3] The abbreviations used are: PcP, *Pneumocystis* pneumonia; TMP, trimethoprim; SMX, sulfamethoxazole; TNF, tumor necrosis factor; BALF, bronchoalveolar lavage fluid; ODC, ornithine decarboxylase; SRM, spermidine synthase; SMS, spermine synthase; SSAT, spermidine/spermine N^1-acetyltransferase; PAO, polyamine oxidase; SMO, spermine oxidase; OAZ, ODC antizyme; Dex, dexamethasone; PBS, phosphate-buffered saline; DMEM, Dulbecco's modified Eagle's medium; RT, reverse transcription; HRP, horseradish peroxidase; SPD, spermidine; PE, phycoerythrin; siRNA, small interference RNA; IHC, immunohistochemical; FITC, fluorescein isothiocyanate; TUNEL, terminal deoxynucleotidyl transferase-mediated dUTP nick end labeling; ELISA, enzyme-linked immunosorbent assay; FAM, fluorophore 5-(and-6)-carboxyl fluorescein succinimidyl ester; AZI, antizyme inhibitor.

midine, and N^1-acetylspermine are greatly increased in alveolar macrophages and in the alveoli during PcP (11). We have also found that bronchoalveolar lavage fluid (BALF) obtained from *Pneumocystis*-infected animals can induce normal macrophages to undergo apoptosis and that polyamine levels in BALF from animals with PcP are high (11). This BALF-induced alveolar macrophage apoptosis is diminished when the polyamines in the BALF are depleted and regained when polyamines are added back to the polyamine-depleted BALF (11). These data indicate that polyamines induce alveolar macrophage to undergo apoptosis during PcP.

Polyamines are polycationic amines present in all cells. The most common biological polyamines are putrescine, spermidine, and spermine. Ornithine decarboxylase (ODC) is the key enzyme in polyamine biosyntheses. ODC decarboxylates ornithine to putrescine, which is converted to spermidine by spermidine synthase (SRM). Spermidine is then converted to spermine by spermine synthase (SMS). Polyamine catabolism is activated in response to the increased intracellular polyamine levels to maintain the cellular polyamine homeostasis (14). This catabolism is mediated by spermidine/spermine N^1-acetyltransferase (SSAT), polyamine oxidase (PAO), and spermine oxidase (SMO). SSAT acetylates spermidine to N^1-acetylspermidine and spermine to N^1-acetylspermine. N^1-Acetylspermine and N^1-acetylspermidine are excreted from cells or converted back to spermidine and putrescine, respectively, by PAO, whereas spermine can be back converted to spermidine by SMO. The catabolic reactions of PAO and SMO are accompanied by the generation of H_2O_2, a reactive oxygen species that can induce apoptosis (15).

Polyamines are involved in the regulation of many cellular functions, such as cell cycle progression (16), differentiation (17), oncogenesis (18), and apoptosis (19). Polyamines mediate G_1 to S phase transition in the cell cycle by increasing the expression of cyclin A, which binds to cyclin-dependent kinase 2. The cyclin A-cyclin-dependent kinase 2 complex increases the rate of DNA synthesis during cell proliferation (16). A number of studies have demonstrated the essential role of polyamine in cell differentiation, but the mechanisms are not clear (17, 20, 21). The role of polyamines in cancer formation has been extensively studied, and a number of polyamine-mediated oncogenesis mechanisms have been reported (18, 22). For example, the oncoprotein c-Myc activates the expression of ODC, which produces polyamines to stimulate cell proliferation (22). Another oncoprotein, K-*ras*, inhibits polyamine catabolism by suppressing the transcription of SSAT, resulting in the accumulation of intracellular polyamines that cause increased cell proliferation and development of neoplasia (18).

In addition to transcriptional activation by c-Myc, ODC activity is also regulated at the level of protein degradation. ODC antizyme (OAZ) binds to and promotes transport of ODC to the 26 S proteasome for degradation by a ubiquitin-independent mechanism. In contrast, AZI prevents ODC from degradation by binding to OAZ. OAZ and AZI also regulate polyamine transport. Overexpression of OAZ decreases polyamine import (23), whereas AZI overexpression increases polyamine import (24). The mechanisms of OAZ- and AZI-mediated polyamine transport are still unknown.

In this study, we investigated the host sources of polyamines during PcP. The mechanisms by which polyamine levels are increased in alveolar macrophages were also examined. The results showed that inflammatory cells present in the lung during PcP are sources of polyamines and that the increase in intracellular polyamine levels in alveolar macrophages are due to both *de novo* synthesis of polyamines and increased uptake of exogenous polyamines.

EXPERIMENTAL PROCEDURES

Rat PcP Model—*Pneumocystis carinii* infection in rats was established as described previously (25). Briefly, female Sprague-Dawley rats (Harlan, Indianapolis, IN) of 120–140 g were divided into three groups designated Normal, Dex, and Dex-Pc. Normal rats were immunocompetent and uninfected. Dex rats were treated continuously with 1.8 mg/liter dexamethasone in drinking water to reduce the number of CD4+ T lymphocytes, mimicking the immunosuppression status in AIDS patients. Dex-Pc rats were immunosuppressed with dexamethasone and transtracheally inoculated with 7.5×10^6 *Pneumocystis* trophozoites 1 week after initiation of immunosuppression. To prevent other opportunistic infections, 10,000 units of penicillin (Butler, Dublin, OH) was given intramuscularly each week to each Dex and Dex-Pc rat. This antibiotic had no adverse effects on the growth of *Pneumocystis* organisms in infected rats. It took ~8 weeks for Dex-Pc rats to develop severe *Pneumocystis* pneumonia after inoculation. When Dex-Pc rats were agonal, they were sacrificed for experiments. Age-matched Normal rats were used as controls, while age-matched Dex rats were used to control for the effects of the steroid treatment. Giemsa staining of lung impression smears was performed to determine the existence of *Pneumocystis* and other microorganisms. Dex-Pc lungs were excluded if they contained other microorganisms. All animal studies were approved by the Indiana University Animal Care and Use Committee and supervised by veterinarians.

Isolation of Alveolar Macrophages—To perform bronchoalveolar lavage, rats were first anesthetized by intramuscular injection of a 0.1-ml ketamine mixture (80 mg/ml ketamine hydrochloride, 0.38 mg/ml atropine, and 1.76 mg/ml acepromazine) and then sacrificed. The thoracic cavity and trachea were exposed by dissection. BALF was obtained by instilling 5 ml of sterile phosphate-buffered saline (PBS) into rat lungs via a 14-gauge angiocatheter (BD Biosciences, Bedford, MA) and then recovering the fluid. In experiments using BALF as supplement in cell cultures, Dulbecco's modified Eagle's medium (DMEM) instead of PBS was used for lavage. To isolate alveolar macrophages, multiple lavages were performed until a total of 50 ml of BALF was obtained. The cells in this 50-ml BALF were pelleted by centrifugation at $300 \times g$ for 10 min and then resuspended in 5 ml of DMEM. Alveolar macrophages were isolated by adherence on plastic tissue culture dishes at 37 °C with 5% CO_2 for 1 h followed by washing with warm PBS three times to remove unattached cells. The purity of alveolar macrophages was >97% as determined by anti-reactive macrophage antigen staining described previously (10, 11).

Real-time RT-PCR—Total RNA was isolated using the TRIzol reagent (Invitrogen) according to the manufacturer's

instructions. Reverse transcription was done using the iScript cDNA synthesis kit (Bio-Rad) with a thermal condition of 25 °C for 2 min, 42 °C for 30 min, and 85 °C for 5 min. RNA (0.2 μg) from each sample was reverse transcribed to cDNA, and 2 μl of each cDNA product was used as the template for real-time PCR. Real-time PCR analyses for expression of rat ODC, SSAT, SRM, OAZ, and AZI genes were performed using the Assays-on-Demand gene expression kits (Applied Biosystems, Foster City, CA); each of which contained two primers and a FAM-labeled probe. The mRNA levels of the ribosomal protein S8 gene was determined in an identical manner to serve as the internal control, because its expression is not affected by immunosuppression or infection (8). The primers and probe used for the rat ribosomal protein S8 real-time RT-PCR were described previously (8). Real-time PCR reactions were performed with a TaqMan Universal PCR Master Mix (Applied Biosystems) on a Smartcycler (Cepheid, Sunnyvale, CA) using the following temperature cycling conditions: 50 °C for 2 min, 95 °C for 10 min, and 40 cycles of 92 °C for 15 s and 60 °C for 1 min.

Western Blotting—Alveolar macrophages adhered in one well of a 6-well plate ($\sim$2 $\times$ 10^6 cells) were scraped in 100 μl of cold (4 °C) cell lysis buffer (150 mM NaCl, 1.0% Triton X-100, 1% deoxycholate, 5 mM EDTA, 10 mM Tris, pH 7.2) containing 1% protease inhibitor mixture (Sigma #P8340). Protein samples for Western blot analysis were prepared by adding NuPAGE LDS Sample Buffer (Invitrogen) and NuPAGE Sample Reducing Agent (Invitrogen) to the cell lysates to a final concentration of 1 $\times$ of each reagent and then boiling for 5 min. Proteins in each sample were electrophoresed in a 10% polyacrylamide gel and then transferred onto a polyvinylidene difluoride membrane using the NuPAGE System (Invitrogen). Membranes were blocked by soaking in a buffer containing 3% bovine serum albumin, 0.9% NaCl, 100 mM Tris-HCl (pH 7.6) at 25 °C for 1 h and then reacted with the primary antibody anti-ODC (Lab Vision, Fremont, CA), anti-SSAT (Novus Biologicals, Littleton, CO), anti-OAZ (26, 27), anti-AZI (28), anti-cleaved or activated caspase 3 (Cell Signaling, Danvers, MA), or anti-glyceraldehyde-3-phosphate dehydrogenase (Research Diagnostics, Flanders, NJ) in blocking buffer for 2 h. After washing with TBST (100 mM Tris-HCl, 0.9% NaCl, 0.1% Tween 20, pH 7.6) six times, the blots were reacted with a secondary antibody anti-mouse IgG or anti-rabbit IgG conjugated with horseradish peroxidase (HRP) for 1 h at 25 °C followed again by six washes with TBST. The reaction signals on the blots were developed by chemiluminescence with the ECL Plus reagent kit (Amersham Biosciences) and revealed by exposing the blots to an x-ray film. Densitometry analysis of results on x-ray films was performed by using National Institutes of Health ImageJ (rsb.info.nih.gov/ij/).

Fluorescence Labeling of Spermidine—Labeling of spermidine with fluorescein was performed as previously described (29) with modifications. Due to poor stability in solution, the fluorophore 5-(and-6)-carboxyl fluorescein succinimidyl ester (FAM) (Invitrogen) was freshly prepared in DMSO at a final concentration of 100 mM immediately before use. Spermidine was dissolved in 200 mM NaHCO$_3$ (pH 8.3) to a final concentration of 2 mM. The labeling reaction was performed by mixing 20 μl of FAM with 1 ml of spermidine in a 2-ml Eppendorf tube.

The tube was fastened on a vortexer and shaken for 1 h at room temperature. The labeled products were separated by electrophoresis in a 1% agarose gel in 40 mM 2-(*N*-morpholino)ethanesulfonic acid monohydrate buffer (pH 6.0) at 100 V for 1 h and then visualized by UV transillumination. The FAM-labeled spermidine (FAM-SPD) moved toward the anode and exhibited an extra band in the gel as compared with the sample containing FAM only. The portion of the gel containing FAM-SPD or FAM was excised, chopped to small cubes, and placed at −80 °C until completely frozen. FAM-SPD was recovered by centrifugation at 10,000 $\times$ *g* for 2 h at 4 °C. Additional centrifugations were performed if the gel was not completely thawed. The concentration of recovered FAM-SPD was determined by spectrophotometry at 494 nm using known concentrations of FAM as standards. The yield of FAM-SPD was ≥30 μM. Purified FAM-SPD was stored in small aliquots at −80 °C until use.

Polyamine Uptake Assay—For *in vivo* polyamine uptake assay, each Normal, Dex, and Dex-Pc rat was anesthetized with 100 μl of ketamine mixture intramuscularly and then transtracheally instilled with 200 μl of 5 μM FAM-SPD or FAM. Alveolar macrophages were then isolated as described above 1 h after FAM-SPD or FAM instillation. The cells were mounted on slides in a mounting medium containing 4′,6-diamidino-2-phenylindole to stain the nuclei. The macrophages that took up FAM-SPD were detected and enumerated by fluorescence microscopy. To examine polyamine uptake in *Pneumocystis*-infected lungs, frozen lung sections of FAM-SPD-instilled rats were used. The lungs were first lavaged with 2 ml of PBS three times to remove free FAM-SPD or FAM and then instilled with 2 ml of OCT compound (Sakura, Tokyo, Japan) via a 14-gauge angiocatheter. Each lung was then placed in a base mold filled with OCT and frozen at −80 °C. The frozen lungs were sectioned with a cryostat microtome, and the sections were stored at −80 °C until use. Frozen lung sections were air-dried for 15 s and fixed in acetone for 2 min before staining. After an incubation in 5% bovine serum albumin for 1 h, the lung sections were reacted with phycoerythrin (PE)-conjugated anti-CD68 antibody in 5% bovine serum albumin in PBS for 1 h to stain macrophages followed by three washes with PBS. The nuclei were counterstained with 4′,6-diamidino-2-phenylindole, and the stained slides were examined by fluorescence microscopy. The polyamine uptake assay was also performed in isolated alveolar macrophages after AZI siRNA knockdown. This *ex vivo* polyamine uptake assay was performed by incubating alveolar macrophages with 2.5 μM FAM-SPD in serum-free DMEM for 1 h followed by fluorescence microscopy described above.

Immunohistochemical Staining—Rat lungs were fixed in 4% paraformaldehyde overnight and then embedded in paraffin. Tissue sections on slides were processed for immunohistochemical (IHC) staining by boiling the deparaffinized sections in High pH Target Retrieval Solution (DAKO, Carpinteria, CA) for 20 min to expose hidden antigens. After three PBS washes, sections were immersed in 3% hydrogen peroxide for 5 min to deplete the endogenous peroxidase activity. Immunostaining was performed using the UltraVision LP System with HRP Polymer (Lab Vision). Briefly, sections were incubated in 1% bovine serum albumin in PBS for 30 min followed by antibody staining at room temperature for 2 h. Monoclonal antibodies

against rat ODC (MP16 –2), CD68 (KP1), CD79a (HM47/A9), and CD3ζ (6B10) were purchased from Lab Vision, whereas polyclonal anti-spermidine antibody was acquired from Abcam (Cambridge, MA). The anti-spermidine antibody also cross-reacts with spermine, according to the manufacturer. Primary Antibody Enhancer and HRP polymer were used according to the manufacturer's instructions. Final chromogenic reaction was performed with the metal enhanced DAB substrate (Pierce).

Flow Cytometry—Isolation of single cells from *Pneumocystis*-infected rat lungs was performed as described previously (30). Each anesthetized rat was perfused with 30 ml of cold Dulbecco's PBS via the right ventricle. A total of 5 ml of Dispase II (neutral protease, 5 mg/ml, Sigma) was transtracheally injected into the lungs, and the trachea was ligated with suture silk to avoid leakage. Lungs containing Dispase II were incubated in Dulbecco's PBS for 45 min at 37 °C. The lungs were then cut into small pieces and incubated in 5 ml of Dulbecco's PBS containing 1 mg/ml collagenase/Dispase (Roche Applied Science) and 0.08 mg/ml DNase I Type II (Sigma) for 10 min at 37 °C with shaking. Digested lungs were forced through an 18-gauge needle 10 times and then mixed with 2 ml of fetal bovine serum. Single cells were isolated by filtering through a 70-μm nylon mesh and collected by centrifugation at $300 \times g$ for 10 min. The pelleted cells were treated with 2 ml of red blood cell lysis buffer (Sigma) to remove red blood cells, followed by washing with 10 ml of PBS two times and then enumerated with a hemocytometer. Approximately one million cells were used for each flow cytometric analysis. Fluorescein isothiocyanate (FITC)-conjugated anti-ODC antibody was made by using the FITC Microscale Protein Labeling Kit (AnaSpec, San Jose, CA). PE-conjugated antibodies against CD4, CD8, and CD45RA were purchased from Cedarlane (Burlington, NC). PE-conjugated anti-CD68 antibody was acquired from AbD Serotec (Raleigh, NC). FITC- and PE-conjugated mouse IgG$_1$ antibodies were used as isotype controls. The stained cells were analyzed with a FACScan flow cytometer (BD Biosciences), and the data were interpreted by using BD Biosciences CellQuest Software.

AZI Knockdown with siRNA—The rat AZI siRNA duplex and scrambled siRNA were synthesized by Integrated DNA Technologies (Coralville, IA). The sequence of the AZI siRNA was AAGAUCGUGAAGAAGCACAGU, which has been shown to be effective against AZI expression (31). To perform siRNA knockdown, $\sim 2 \times 10^6$ alveolar macrophages were placed in a well of a 6-well plate containing 2 ml of serum-free DMEM. The cells were transfected with the siRNAs by adding 2 μl of 1 μg/μl of siRNA molecules and 5 μl of TransMessenger (Qiagen) to the well. After 6 h of incubation at 37 °C with 5% CO$_2$, the culture medium was supplemented with a final concentration of 10% fetal bovine serum, 1% antibiotic mixture (Sigma #P4333), and 2 ml of DMEM-based BALF to mimic the original lung environment. The cells were harvested after 3 days of incubation for real-time RT-PCR, Western blotting, and polyamine uptake assays described above.

TUNEL Assay—The TUNEL assay was performed using the DeadEnd Fluorimetric TUNEL System (Promega, Madison, WI) according to the manufacturer's instructions. Apoptotic cells were detected and enumerated by fluorescence microscopy with 4′,6-diamidino-2-phenylindole counterstaining.

Cytosolic Cytochrome c Assay—Determination of cytosolic cytochrome c levels was performed as described previously (11). Briefly, 2×10^6 alveolar macrophages were lysed, and the protein concentrations in the cell lysate were determined by the Bradford protein assay method (Bio-Rad). A total of 5 μg of protein in 100 μl of blocking buffer was used to determine the levels of cytochrome c by the Function ELISA cytochrome c assay kit (Active Motif, Carlsbad, CA). This kit uses the Sandwich ELISA technique with the first antibody to capture and the biotin-conjugated second antibody coupled with HRP-conjugated streptavidin to quantify cytochrome c.

PAO and SMO Activity Assay—PAO activity was assayed by the method of Suzuki *et al.* (32), which measures the levels of H$_2$O$_2$ formed. H$_2$O$_2$ converts homovanillic acid to a fluorescent compound in the presence of HRP. Alveolar macrophages ($\sim 2 \times 10^6$ cells) from each rat were suspended in 1 ml of 83 mM sodium borate (pH 9.0) and broken up by passing through a 1-ml syringe with a 25-gauge needle 20 times. 500 μl of cell lysate was preincubated with 5 units of HRP for 20 min at 37 °C to remove endogenous substrates of hydrogen peroxide-producing enzymes. 100 μg of homovanillic acid and N^1-acetyl-spermine (final concentration, 250 μM) were then added followed by an incubation at 37 °C for 30 min. The PAO reaction was stopped by adding 1 ml of 0.1 M NaOH solution. The intensity of fluorescence generated in the reaction was measured by fluorometry with an excitation wavelength of 323 nm and emission wavelength of 426 nm. Protein concentration was determined with a Bradford protein assay dye (Bio-Rad), and PAO activity was shown in the amount H$_2$O$_2$ produced per min per mg of protein. SMO activity was measured by the same method except that the substrate was replaced by spermine.

Statistical Analysis—Data are presented as means $\pm$ S.D. with the indicated number of experiments. The two-tailed Student's t test was used for statistical analysis, and the difference between the two groups analyzed was considered statistically significant if the p value was <0.05.

RESULTS

Polyamine Synthesis in Alveolar Macrophages during PcP—To examine whether the increased polyamine levels in alveolar macrophages during PcP are due to increased polyamine synthesis, the expression levels of ODC, SSAT, and SRM were determined by real-time RT-PCR and Western blotting. The results showed that the mRNA levels of ODC, SSAT, and SRM in alveolar macrophages from immunosuppressed (Dex) rats were 0.93-, 1.54-, and 1.21-fold, respectively, of those of Normal rats (data not shown). Because these differences were not statistically significant, the results indicated that long term treatment of rats with dexamethasone did not significantly affect polyamine synthesis mediated by ODC, SSAT, or SRM. In alveolar macrophages from Dex-Pc rats, ODC, SSAT, and SRM mRNA levels were 1.01-, 0.94-, and 1.01-fold that of Dex rats (data not shown), indicating that *Pneumocystis* infection also did not significantly affect the transcription of these genes. Western blotting analysis revealed that the level ODC protein in alveolar macrophages was not changed by immunosuppression but was increased $\sim$8-fold during *Pneumocystis* infection (Fig. 1). In contrast, the SSAT protein level was not altered

during *Pneumocystis* infection (Fig. 1). The protein level of SRM was not determined, because anti-rat SRM antibody was not commercially available. The change in ODC protein but not mRNA levels indicated that ODC expression was regulated by a
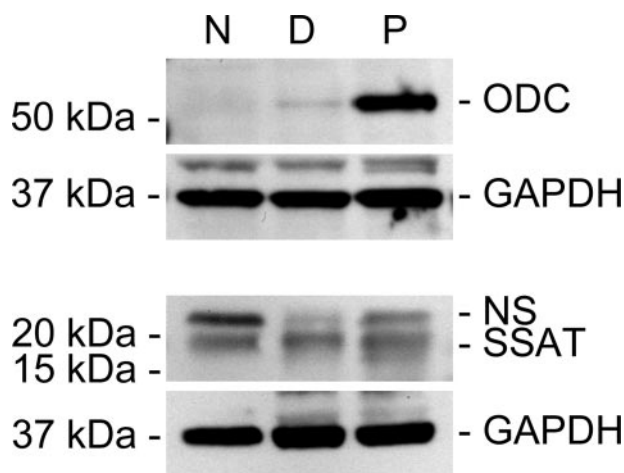

FIGURE 1. **Expression of polyamine synthesis enzymes in alveolar macrophages.** Protein levels of ODC and SSAT in alveolar macrophages were analyzed by Western blotting. Results shown are representative of three independent experiments. *N*, normal rats; *D*, Dex rats; *P*, Dex-Pc rats; and *NS*, nonspecific band.
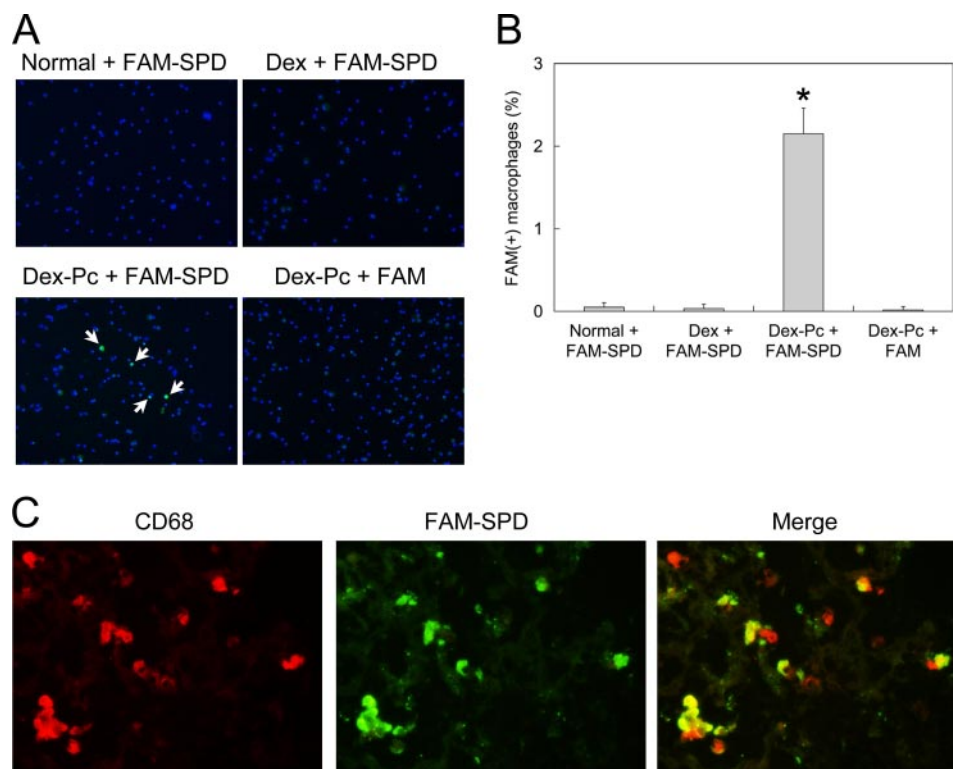

FIGURE 2. **Polyamine uptake assay.** *A*, 200 μl of 5 μM FAM-SPD or FAM was transtracheally instilled into Normal, Dex, and Dex-Pc rats. Alveolar macrophages were isolated 1 h after the instillation and examined by fluorescence microscopy. *Arrows* indicate the cells with internalized FAM-SPD. *B*, a total of 1000 randomly selected cells of each sample shown in *A* were counted, and the percentages of cells with internalized FAM or FAM-SPD were determined and diagrammed. Results represent mean $\pm$ S.D. from four experiments. *, $p < 0.05$ as compared with Dex control. *C*, Dex-Pc rats were transtracheally instilled with FAM-SPD. 1 h after the instillation, rats were sacrificed, and frozen lung sections were made and stained for the macrophage marker CD68. *Merged images* show that the cells that took up FAM-SPD were exclusively alveolar macrophages, because every cell that took up polyamine was CD68-positive, and no CD68-negative cells took up polyamines.

post-transcriptional mechanism in alveolar macrophages during PcP.

Polyamine Uptake by Alveolar Macrophages during PcP—Elevated intracellular polyamine levels could also be due to increased polyamine uptake; therefore, polyamine uptake assays were performed. Purified FAM-labeled spermidine (FAM-SPD) was transtracheally instilled into the lungs of Normal, Dex, and Dex-Pc rats. One hour after the transtracheal instillation, rats were sacrificed and lavaged to obtain alveolar macrophages. Fluorescence microscopy showed that <0.1% of alveolar macrophages from Normal and Dex rats but greater than 2% of those from Dex-Pc rats contained FAM-SPD (Fig. 2*A*), suggesting that the number of alveolar macrophages that can take up exogenous polyamines was increased by ~20-fold during PcP (Fig. 2*B*). To confirm that these cells took up FAM-SPD and not FAM nonspecifically, a separate group of Dex-Pc rats were transtracheally instilled with FAM. This experiment revealed that <0.1% alveolar macrophages in this group of rats internalized FAM (Fig. 2*B*), confirming the specificity of polyamine uptake. To identify the cells that took up polyamines, frozen lung sections from FAM-SPD-instilled Dex-Pc rats were stained for the macrophage marker CD68, and all the cells that contained FAM-SPD were positive for CD68 (Fig. 2*C*), indicating that they were macrophages.

ODC Expression in Rat Lungs during PcP—To determine the sources of polyamines in the lung during PcP, IHC staining for ODC was performed on lung sections from Normal, Dex, and Dex-Pc rats. H&E and ODC staining revealed no differences in the microscopic features of the lungs from Normal and Dex rats, indicating that immunosuppression of rats with dexamethasone had no effect on ODC expression. However, ODC expression in the lung was greatly affected by *Pneumocystis* infection. The ODC protein was not detectable in most pulmonary cells, but was highly expressed in the mononuclear cells located around blood vessels and bronchioles (Fig. 3*A*), suggesting that these inflammatory cells were sources of polyamines during PcP. Interestingly, the intracellular location of ODC was changed during PcP. ODC was found distributed evenly in the cytoplasm of inflammatory cells from uninfected rats, but was located in pericytoplasmic areas in those from infected rats (Fig. 3*A*). To identify these cells, serial lung sections from Dex-Pc rats were stained with cell-specific markers CD68 (monocyte), CD79a (B lymphocyte), and CD3ζ (T lymphocyte). Results showed that these

ODC-positive cells may be monocytes and B or T lymphocytes (Fig. 3*B*). Polyamine production determined by anti-spermidine staining also showed that the cells in this area contain high levels of polyamines (Fig. 3*B*).

Flow Cytometry Analysis of ODC-positive Cells in the Lung with PcP—To quantify and further identify ODC-positive cells, total lung cells isolated from Dex-Pc rats were analyzed by flow cytometry. Anti-ODC antibody was labeled with FITC, and antibodies against CD4, CD8, CD45RA, and CD68 were labeled with PE. In this assay, 24.44% of total lung cells from Dex-Pc rats were ODC-positive (Table 1). Dual staining of the cells with ODC and CD4, CD8, CD45RA, or CD68 antibodies revealed that 1.83% of the cells

were ODC+CD4+, 8.27% were ODC+CD8+, 9.79% were ODC+CD45RA+ (B lymphocytes), and 7.80% were ODC+CD68+ (monocytes/macrophages).

OAZ and AZI Expressions in Alveolar Macrophages during PcP—Because OAZ and AZI have been shown to regulate both polyamine production and transport (23, 24), their expressions in alveolar macrophages from Normal, Dex, and Dex-Pc rats were determined. Real-time RT-PCR results revealed that the mRNA expression levels of OAZ in alveolar macrophages from Dex and Dex-Pc rats were 0.93- and 0.96-fold, respectively, of those of Normal rats (Fig. 4*A*); these differences were not statistically significant. Western blotting results also showed that OAZ protein levels in alveolar macrophages were not affected by immunosuppression or *Pneumocystis* infection (Fig. 4*B*). In contrast, AZI mRNA levels in alveolar macrophages from Dex-Pc rats were 3.16-fold higher than those from Dex rats (Fig. 4*A*), and AZI protein levels in alveolar macrophages were increased by 6-fold during PcP as determined by Western blotting (Fig. 4*B*).

Polyamine Synthesis and Uptake after AZI Knockdown—To correlate AZI overexpression with alveolar macrophage apoptosis during PcP, alveolar macrophages isolated from Dex-Pc rats were analyzed for AZI expression, polyamine synthesis, polyamine uptake, and apoptosis after AZI siRNA knockdown. Results from real-time PCR showed that AZI siRNA successfully decreased AZI mRNA levels by ~70% in alveolar macrophages from Dex-Pc rats (Fig. 5*A*). This AZI knockdown was also found to cause a 60% decrease in ODC protein level in these alveolar macrophages (Fig. 5*B*). In the *ex vivo* spermidine uptake assay, a 50% reduction in the number of cells taking up polyamines was observed in the group of cells transfected with AZI siRNA as compared with control transfectants (Fig. 5*C*).

Macrophage Apoptosis after AZI Knockdown—BALFs from *Pneumocytes*-infected rats have been shown to induce macrophages to undergo apoptosis due to elevated levels of polyamines (11). To determine whether AZI plays a role in this BALF-induced apoptosis, 2×10^6 normal rat alveolar macrophages were transfected with AZI siRNA and then incubated with BALF from Dex-Pc rats 6 h after siRNA transfection. Three days after the transfection and BALF treatment, cells were analyzed for apoptosis by three different methods. Results from TUNEL assay showed that the number of apoptotic cells was decreased by 53% (Fig. 6, *A* and *B*). The levels of cytosolic cytochrome *c* showed a 58% reduction (Fig. 6*C*), and those of activated caspase-3 determined by Western blotting were decreased by 75% in macrophages transfected with AZI siRNA as compared with controls that were transfected with scrambled siRNA (Fig. 6*D*).
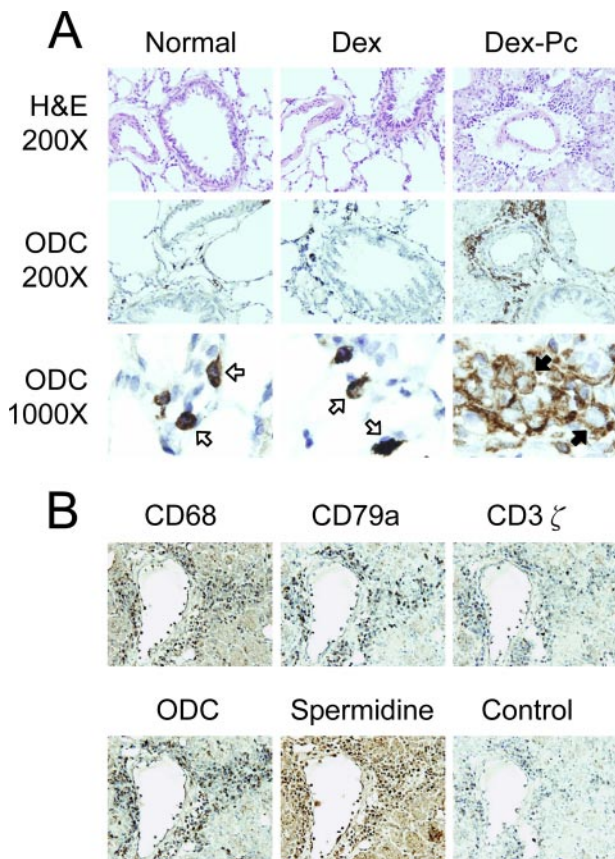

FIGURE 3. **ODC expression in the lung.** *A*, H&E staining (*top*) and IHC staining for ODC were performed on lung sections from Normal, Dex, and Dex-Pc rats. Cells reacted with anti-ODC antibody were examined at the magnifications of 200× (*middle*) and 1000× (*bottom*). *Open* and *solid arrows* indicate the cells with homogenous and pericytoplasmic ODC expression patterns, respectively. Results shown are representative of three sets of animals. *B*, IHC staining for CD68 (monocyte), CD79a (B cell), CD3ζ (T cell), ODC, and spermidine was performed on serial sections from Dex-Pc lungs. The control was processed in an identical manner except that no primary antibody was used. Magnification = 200×.

TABLE 1

Flow cytometry analysis of lung cells from *Pneumocystis*-infected rats

	FITC(−)PE(−)	FITC(−)PE(+)	FITC(+)PE(−)	FITC(+)PE(+)
Isotype control	95.75 ± 0.81	0.04 ± 0.07	2.54 ± 0.10	1.66 ± 0.84
ODC-FITC	73.95 ± 5.43	0.00 ± 0.00	24.44 ± 6.78	1.61 ± 1.34
ODC-FITC + CD4-PE	77.04 ± 4.37	0.07 ± 0.06	21.06 ± 5.40	1.83 ± 1.09
ODC-FITC + CD8-PE	82.07 ± 2.59	0.02 ± 0.01	9.63 ± 1.60	8.27 ± 0.99[a]
ODC-FITC + CD45RA-PE	82.73 ± 1.12	0.77 ± 0.58	6.71 ± 1.37	9.79 ± 1.91[a]
ODC-FITC + CD68-PE	76.73 ± 3.19	0.00 ± 0.01	15.20 ± 8.01	7.80 ± 4.42[a]

[a] $p < 0.05$ compared to the FITC(+)PE(+) quadrant of the ODC-FITC group ($n = 4$).
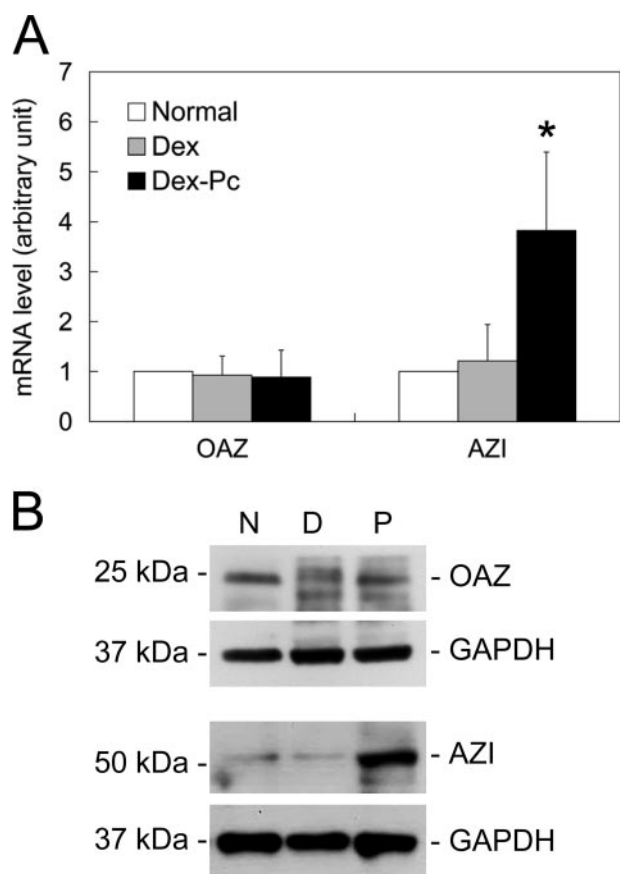
FIGURE 4. **OAZ and AZI expressions in alveolar macrophages.** mRNA and protein levels of OAZ and AZI in alveolar macrophages from Normal (*N*), Dex (*D*), and Dex-Pc (*P*) rats were determined by real-time RT-PCR (*n* = 5) (*A*) and Western blotting (*n* = 3) (*B*). The average mRNA levels of OAZ and AZI genes in alveolar macrophages from Dex and Dex-Pc rats presented in *panel A* are shown as -fold increase relative to those of Normal rats, each of which was arbitrarily set to 1. *, $p < 0.05$ as compared with Dex control.

FIGURE 5. **Polyamine synthesis and uptake after siRNA knockdown of AZI.** *A*, real-time RT-PCR analysis of AZI mRNA levels after siRNA knockdown. Alveolar macrophages from Dex and Dex-Pc rats were transfected with AZI siRNA (*siAZI*) or scrambled siRNA (*Scrambled*) and then measured for AZI mRNA levels. *B*, the ODC protein level in alveolar macrophages from Dex-Pc rats was determined by Western blotting after transfection with AZI siRNA (*siAZI*) or scrambled siRNA (*Scr*). *C*, alveolar macrophages from Dex-Pc rats were assayed for FAM-SPD uptake after transfection with AZI siRNA (*siAZI*) or scrambled siRNA (*Scr*). A total of 1000 cells of each sample was counted, and the percentages of cells with internalized FAM-SPD were determined and diagrammed.

Substances That Induce AZI Overexpression—Because AZI was found overexpressed in alveolar macrophages from Dex-Pc rats, experiments were performed to determine whether certain substances capable of inducing the expression of AZI are present in BALF from Dex-Pc rats. Alveolar macrophages from normal rats were first treated with the BALF and then measured for AZI mRNA by RT-PCR. This treatment resulted in a 1.5-fold increase in AZI mRNA levels in alveolar macrophages compared with the same cells treated with BALF from Dex rats (Fig. 7*A*), suggesting that AZI expression in alveolar macrophages can be induced by a certain substance in *Pneumocystis*-infected lungs. To identify such substance, alveolar macrophages from normal rats were treated with *Pneumocystis* organisms and the cytokine TNF-α, which is present in high levels in *Pneumocystis*-infected lungs. Results showed that *Pneumocystis* organisms but not TNF-α increased AZI mRNA levels in a dose-dependent manner (Fig. 7*B*). The same result was observed when normal rat alveolar macrophages were treated with zymosan A (Fig. 7*B*). These results suggest that a component of the *Pneumocystis* cell wall is responsible for the increase in AZI expression during PcP.

Polyamine Catabolism and Alveolar Macrophage Apoptosis—To investigate whether polyamine catabolism plays a role in alveolar macrophage apoptosis during PcP, the expres-
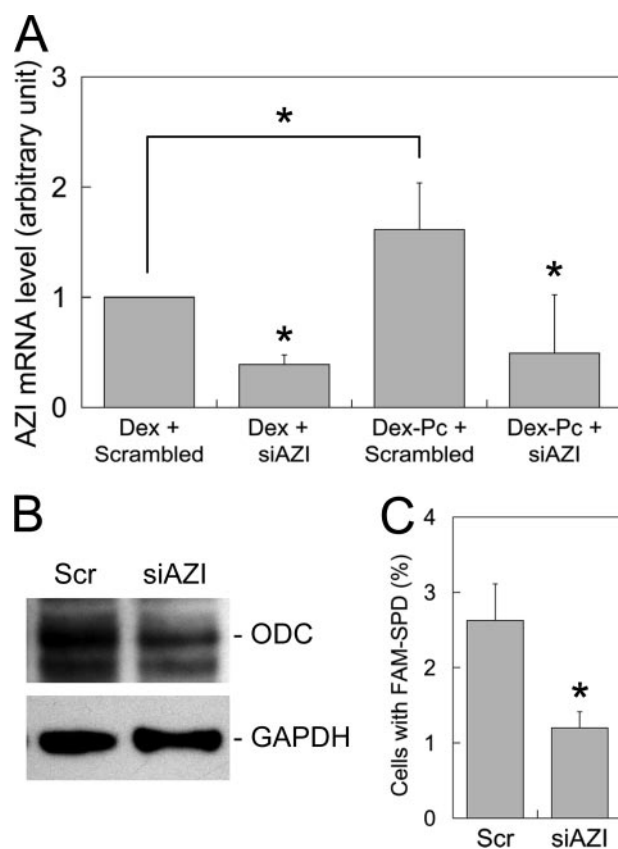
sion and activity levels of PAO and SMO in alveolar macrophages from *Pneumocystis*-infected rats were determined. Results of real-time RT-PCR showed that PAO mRNA levels in alveolar macrophages from Dex-Pc rats were 2.82-fold that of those from Dex rats, but SMO mRNA levels were not significantly changed (Fig. 8*A*). PAO protein levels were found increased ~4-fold in alveolar macrophages during PcP (Fig. 8*B*), and PAO activity in alveolar macrophages from *Pneumocystis*-infected rats showed a 2.24-fold increase as compared with the Dex control (Fig. 8*C*). These results suggest that polyamine oxidation plays a role in alveolar macrophages apoptosis in *Pneumocystis*-infected lungs.

DISCUSSION

We have previously found that the levels of spermidine, N^1-acetylspermidine, and N^1-acetylspermine in both the alveoli and alveolar macrophages are elevated leading to increased rate of alveolar macrophage apoptosis during PcP (11). In the present study, we investigated the possible mechanisms for such increase in polyamine levels. The transcription of the ODC gene, which encodes the key enzyme in polyamine synthesis, in alveolar macrophages was not affected by *Pneumocys-*
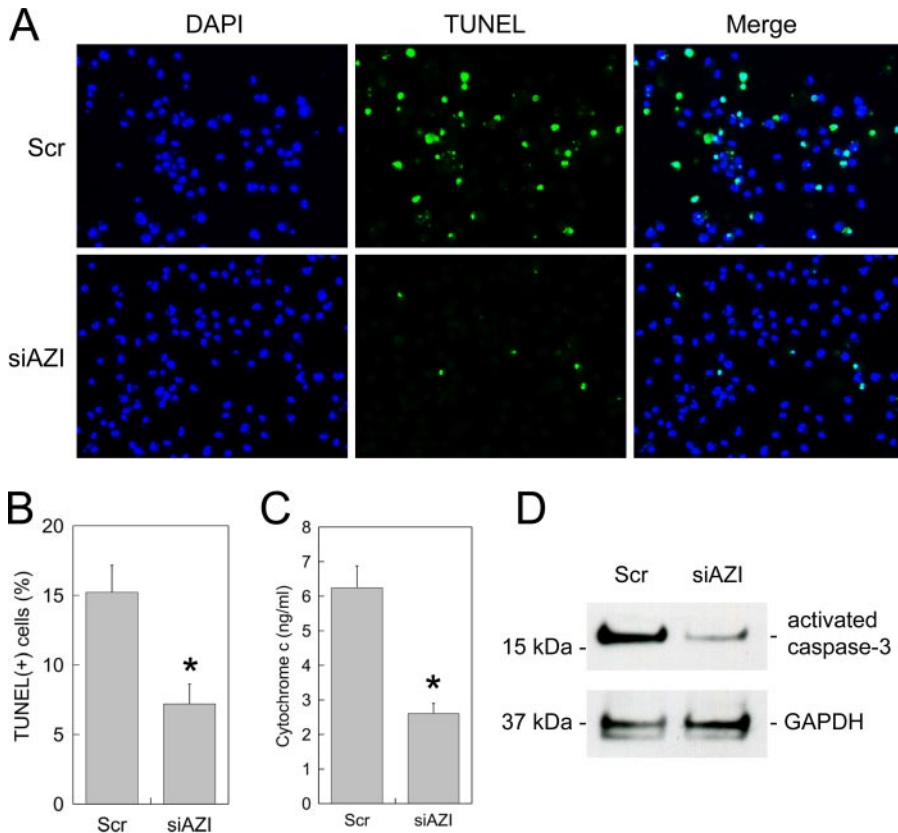
FIGURE 6. **Macrophage apoptosis after siRNA knockdown of AZI.** *A*, Normal rat alveolar macrophages were transfected with AZI siRNA (*siAZI*) or scrambled siRNA (*Scr*) and then treated with BALF from Dex-Pc rats. Three days after transfection, a TUNEL assay was performed, and cells were examined by fluorescence microscopy. *B*, a total of 1000 randomly selected cells of each sample shown in *A* were counted, and the percentages of apoptotic cells were diagrammed. Results represent mean ± S.D. from three experiments. *, $p < 0.05$ as compared with scrambled control. *C*, cytosolic cytochrome *c* levels in cells treated with siRNA and BALF from Dex-Pc rats were measured. Results represent mean ± S.D. from three experiments. *, $p < 0.05$ as compared with scrambled control. *D*, the level of activated caspase-3 in alveolar macrophages from Dex-Pc rats was determined by Western blotting after transfection with AZI siRNA (*siAZI*) or scrambled siRNA (*Scr*).
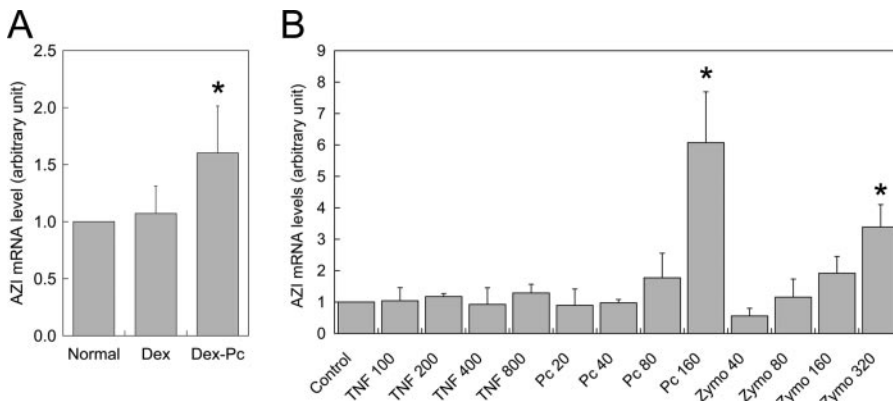

FIGURE 7. **Induction of AZI overexpression.** *A*, Normal rat alveolar macrophages were incubated with Normal, Dex, and Dex-Pc BALF for 24 h and then examined by real-time RT-PCR for AZI expression. Results represent mean ± S.D. from five experiments. *, $p < 0.05$ as compared with the Dex control. *B*, Normal rat alveolar macrophages were incubated with TNF-α (*TNF*, 100–800 pg/μl), *P. carinii* organisms (*Pc*, 20–160 nuclei/μl), or zymosan A (*Zymo*, 40–320 ng/μl) for 18 h and then examined by real-time RT-PCR for AZI expression. Results represent mean ± S.D. from three analyses. *, $p < 0.05$ as compared with mock control.

binds to ODC and transports it to the 26 S proteasome for degradation, whereas AZI competes with ODC for binding to OAZ. When AZI binds to OAZ, less ODC is degraded and thus a steady-state level of polyamines in the cells is maintained. Because OAZ mRNA and protein levels were not changed (Fig. 4) but both the mRNA (3-fold) and protein (6-fold) levels of AZI were greatly increased (Fig. 4), it is likely that the ODC turnover rate in alveolar macrophages during PcP is decreased due to AZI overexpression. The result that AZI knockdown by siRNA decreased the ODC protein level by 60% (Fig. 5*B*) confirmed this possibility. Higher polyamine synthesis during PcP was demonstrated by the IHC experiment in which ODC-positive cells, mainly inflammatory cells, were shown to react with the anti-spermidine antibody (Fig. 3 and Table 1), indicating polyamine synthesis in these cells.

An interesting finding in this study is that ODC distribution in inflammatory cells was changed from cytoplasmic to pericytoplasmic (Fig. 3*A*). ODC translocation has been shown to be associated with cell cycle progression (33) or cell activation and transformation (34). Because inflammatory cells are activated when they are recruited to the lung, it is very likely that the change in ODC distribution is due to cell activation during PcP and that this activation leads to elevated polyamine synthesis.

In addition to increased synthesis, increased uptake of exogenous polyamines is another possible cause of elevated polyamine levels in alveolar macrophages during PcP. However, polyamine transporters in mammalian cells remain largely unknown. Synthetic fluorescent polyamines have been used to explore mammalian polyamine transport systems (35–37), and a receptor-mediated endocytosis mechanism has been suggested (35, 36). Another study showed that polyamine uptake was unaffected in endocytosis-deficient cells and that the internalized polyamines were co-localized with acidic vesicles of the late endocytic compartment and the *trans*-Golgi (37). This

tis infection, but the ODC protein level in alveolar macrophages was greatly (8-fold) increased during PcP (Fig. 1), indicating that the balance between ODC synthesis and degradation is altered during *Pneumocystis* infection. As described above, the ODC protein level is controlled by both OAZ and AZI. OAZ
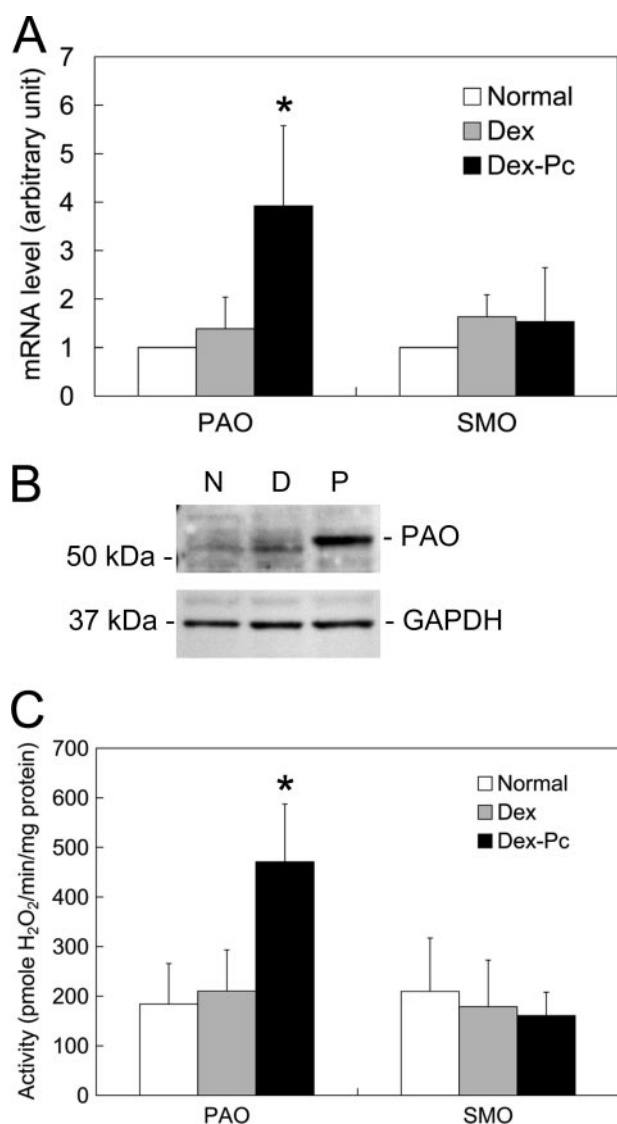
FIGURE 8. **Polyamine catabolism.** *A*, the mRNA levels of PAO and SMO in alveolar macrophages form Normal (*N*), Dex (*D*), and Dex-Pc (*P*) rats were determined by real-time RT-PCR. The average mRNA levels of these genes in alveolar macrophages from Dex and Dex-Pc rats are shown as -fold increase relative to those of Normal rats, each of which was arbitrarily set to 1. Results represent mean $\pm$ S.D. from five experiments. *, $p < 0.05$ as compared with the Dex control. *B*, protein levels of PAO and SMO in alveolar macrophages were analyzed by Western blotting. *C*, the enzyme activities of PAO and SMO in alveolar macrophages from Normal, Dex, and Dex-Pc rats were determined. Results represent mean $\pm$ S.D. from five experiments. *, $p < 0.05$ as compared with Dex control.

finding suggests that polyamines are imported by a membrane carrier (37). The mammalian polyamine transport systems that have been described appear to have a broad substrate specificity and can transport a variety of polyamines (35). Therefore, it is possible that the spermidine uptake system (Fig. 2) is also responsible for the uptake of N^1-acetylspermidine and N^1-acetylspermine into alveolar macrophages during PcP. Polyamine uptake assays are commonly performed using radioactive polyamines (38–40). Aziz *et al.* (41) and Aouida *et al.* (29) used fluorescein-labeled polyamines to perform such assays in cultured cells and yeasts by fluorescence microscopy. It was demonstrated that the fluorescein moiety does not affect the transport of polyamines (41). In this study, we used fluores-

cein-labeled spermidine to investigate polyamine uptake in *Pneumocystis*-infected rats. We also modified Aouida's labeling process to increase the yield and showed for the first time that FAM-labeled spermidine can be used for polyamine uptake assay *in vivo* (Fig. 2).

Although the number of alveolar macrophages that took up fluorescent spermidine (FAM-SPD) in the polyamine uptake assay was found to be 20-fold higher in *Pneumocystis*-infected than in uninfected rats, only ~2% of alveolar macrophages in *Pneumocystis*-infected rats internalized FAM-SPD (Fig. 2*B*). The reason for this low number of cells taking up FAM-SPD is unknown. It may be that most alveolar macrophages in *Pneumocystis*-infected lungs already contain high levels of polyamines (11) and are no longer able to take up exogenous polyamines. The alveolar macrophages that took up FAM-SPD in the polyamine uptake assay were probably those containing lower levels of intracellular polyamines. This possibility remains to be investigated. Because overexpression of AZI has been shown to increase polyamine uptake (24), it is conceivable that the increased level of AZI in alveolar macrophages contributes to this increased uptake of exogenous polyamines. The result that AZI expression knockdown by siRNA decreased the number of cells that can take up polyamines by 50% (Fig. 5*C*) strongly supports this possibility. A likely source of exogenous polyamines is *Pneumocystis* organisms, because they have been shown to produce and secrete polyamines, mainly N^1-acetylspermine and N^1-acetylspermidine (42). Because SSAT levels were not increased in alveolar macrophage during PcP (Fig. 1), the elevated levels of acetylated polyamines in alveolar macrophages are more likely due to uptake of such polyamines from exogenous sources. Like SSAT, the expression level of the spermidine synthase (SRM), which converts putrescine to spermidine, was also not increased in alveolar macrophage during PcP (data not shown), suggesting that SRM is not responsible for the increased spermidine level. It is possible that the increased spermidine level was due to conversion of N^1-acetylspermine to spermidine.

In addition to *Pneumocystis* organisms, we believe that inflammatory cells are another source of polyamines, because they stained positively for ODC, and spermidine levels were high in these cells (Fig. 3*B* and Table 1). These cells were mainly located around blood vessels and bronchioles (Fig. 3*A*) and therefore are considered inflammatory cells that were recruited into the lung during PcP. Approximately 25% of the total lung cells from infected rats were ODC-positive. These inflammatory cells were shown by flow cytometry to be CD4+ T cells (1.83%), CD8+ T cells (9.79%), B cells (9.79%), and CD68+ cells (7.80%) that may be monocytes or macrophages. In this study, ODC was found to be present only in inflammatory cells by IHC staining (Fig. 3) and flow cytometry (Table 1), indicating that ODC levels were higher in inflammatory cells than in other types of pulmonary cells. The uninfected lungs were not analyzed for ODC-positive cells, because very few inflammatory cells were present.

Conversion of N^1-acetylspermine to spermidine and N^1-acetylspermidine to putrescine by PAO is accompanied by the production of H_2O_2 which may damage mitochondria leading to induction of apoptosis. This mechanism is thought to be

responsible for the loss of alveolar macrophages during PcP, because reactive oxygen species levels are increased in alveolar macrophages during PcP (11). Because the mRNA, protein expression, and enzymatic activity levels of PAO were all found to be increased in alveolar macrophages during PcP (Fig. 8), it is conceivable that the reactive oxygen species generated by PAO plays an important role in alveolar macrophage apoptosis during *Pneumocystis* infection. It is possible that PAO overexpression in alveolar macrophages during PcP is induced by the increased intracellular levels of PAO substrates N^1-acetylspermidine and N^1-acetylspermine (11). An important finding in this study is that AZI expression knockdown by siRNA resulted in a 53% decrease in the number of apoptotic alveolar macrophages (Fig. 6*B*), a 58% decrease in cytosolic cytochrome *c* levels (Fig. 6*C*), and a 75% decrease in the level of activated caspase-3 (Fig. 6*D*). This result indicates that decreasing AZI protein levels also decreases the apoptosis rate of alveolar macrophages. It is possible that the reduction in AZI levels causes a decreased uptake of exogenous acetylated polyamines; therefore, less acetylated polyamines are available to be converted to regular polyamines, and thus less H_2O_2 is produced to trigger apoptosis. This is the first demonstration that AZI is involved in apoptosis. A previous study showed that transfection of the gene encoding OAZ, the negative regulator of AZI, can also induce apoptosis by activating mitochondrial depolarization and caspase cascade (43). It is not surprising that both OAZ and AZI have a pro-apoptotic activity due to the multiple roles of polyamines (18, 19).

Polyamines have also been found to be involved in the pathogenesis of *Helicobacter pylori*. *H. pylori* activates the transcriptional factor c-Myc, which induces ODC expression, resulting in increased intracellular polyamine pools in macrophages (44). This polyamine accumulation greatly reduces the uptake of L-arginine, which is the substrate of inducible nitric oxide synthase and is also the rate-limiting factor for inducible nitric oxide synthase translation (45). Therefore, increased polyamine levels consequently decrease the synthesis of inducible nitric oxide synthase in macrophages and result in loss of innate immune responses against *H. pylori* infection (46). *H. pylori* also activates SMO to convert spermidine to spermine accompanied by generation of H_2O_2, which causes macrophages to undergo apoptosis (15, 47). Therefore, induction of apoptosis by polyamines appears to be a survival mechanism for microbes to evade the clearance by immune systems.

Although both *Pneumocystis* and *H. pylori* cause macrophages to undergo apoptosis due to elevated levels of polyamines, the mechanisms in polyamine acquisition are different. Unlike *H. pylori*, *Pneumocystis* does not up-regulate ODC synthesis. Instead, it up-regulates AZI expression leading to increased uptake of exogenous polyamines and decreases the degradation of ODC thus increasing polyamine synthesis. Therefore, the increase in polyamine levels in alveolar macrophages during PcP is due to both increased uptake and polyamine synthesis. Up-regulation of AZI expression has also been shown in other diseases. A comparative clinical study showed that gastric cancer tissue removed during surgery expresses higher levels of AZI than the surrounding normal tissue (48). Oncogene Ras-transformed NIH3T3 cells also have increased

AZI expression (24). Although AZI levels have been shown to be induced in a number of conditions, the mechanisms for AZI overexpression were largely unknown. In this study, we found that both *Pneumocystis* organisms and zymosan A induced AZI expression in a dose-dependent manner (Fig. 7*B*). Because the major component of zymosan A is β-glucan, which is also the major component of the *Pneumocystis* cell wall, it is very likely that β-glucan induces AZI overexpression in alveolar macrophages. The dectin-1 receptor has been shown to be the main receptor for β-glucan on alveolar macrophages (49), and binding of β-glucan to dectin-1 has been shown to activate the NF-κB signaling pathway (50). Therefore, it is possible that AZI expression is regulated by NF-κB. This possibility is being investigated. Because increased polyamine levels due to both increased synthesis and uptake are responsible for the apoptosis of alveolar macrophages during PcP, decreasing polyamine synthesis, uptake, or both may be potential therapeutic approach for PcP, because we have shown that prevention of alveolar macrophage apoptosis reduced the severity of PcP (13). Difluoromethylornithine, one of the most effective ODC inhibitors, has been used to treat rats with PcP, and the results showed that difluoromethylornithine decreases organism counts, although it was not as effective as TMP-SMX (51, 52). This partial success may be due to the compensatory effects of polyamine uptake. Recently, a synthetic compound, referred to as compound #7, has been shown to inhibit polyamine import with very low cytotoxicity (53). This type of polyamine transport inhibitor may be used alone or in combination with difluoromethylornithine for therapy of PcP by decreasing the intracellular polyamine levels and apoptosis rate of alveolar macrophages.

REFERENCES

1. Phair, J., Munoz, A., Detels, R., Kaslow, R., Rinaldo, C., and Saah, A. (1990) *N. Engl. J. Med.* **322,** 161–165
2. Huang, L., Crothers, K., Atzori, C., Benfield, T., Miller, R., Rabodonirina, M., and Helweg-Larsen, J. (2004) *Emerg. Infect. Dis.* **10,** 1721–1728
3. Nahimana, A., Rabodonirina, M., Bille, J., Francioli, P., and Hauser, P. M. (2004) *Antimicrob. Agents Chemother.* **48,** 4301–4305
4. Stein, C. R., Poole, C., Kazanjian, P., and Meshnick, S. R. (2004) *Emerg. Infect. Dis.* **10,** 1760–1765
5. Limper, A. H., Hoyte, J. S., and Standing, J. E. (1997) *J. Clin. Invest.* **99,** 2110–2117
6. Ezekowitz, R. A. B., Williams, D. J., Koziel, H., Armstrong, M. Y., Warner, A., Richards, F. F., and Rose, R. M. (1991) *Nature* **351,** 155–158
7. Steele, C., Marrero, L., Swain, S., Harmsen, A. G., Zheng, M., Brown, G. D., Gordon, S., Shellito, J. E., and Kolls, J. K. (2003) *J. Exp. Med.* **198,** 1677–1688
8. Zhang, C., Wang, S. H., Lasbury, M. E., Tschang, D., Liao, C. P., Durant, P. J., and Lee, C. H. (2006) *Infect. Immun.* **74,** 1857–1864
9. Fleury, J., Escudier, E., Pocholle, M. J., Carre, C., and Bernaudin, J. F. (1985) *Acta Cytol.* **29,** 721–726
10. Lasbury, M. E., Durant, P. J., Bartlett, M. S., Smith, J. W., and Lee, C. H. (2003) *Clin. Diagn. Lab. Immunol.* **10,** 293–302
11. Lasbury, M. E., Merali, S., Durant, P. J., Tschang, D., Ray, C. A., and Lee, C. H. (2007) *J. Biol. Chem.* **282,** 11009–11020
12. Lasbury, M. E., Durant, P. J., and Lee, C. H. (2003) *J. Eukaryot. Microbiol.* **50,** (suppl.) 630–631
13. Lasbury, M. E., Durant, P. J., Ray, C. A., Tschang, D., Schwendener, R., and Lee, C. H. (2006) *J. Immunol.* **176,** 6443–6453
14. Wang, Y., and Casero, R. A., Jr. (2006) *J. Biochem.* (*Tokyo*) **139,** 17–25
15. Chaturvedi, R., Cheng, Y., Asim, M., Bussiere, F. I., Xu, H., Gobert, A. P.,

Hacker, A., Casero, R. A., Jr., and Wilson, K. T. (2004) *J. Biol. Chem.* **279,** 40161–40173

16. Oredsson, S. M. (2003) *Biochem. Soc. Trans.* **31,** 366–370
17. Verma, D. S., and Sunkara, P. S. (1982) *Cancer Res.* **42,** 3046–3049
18. Gerner, E. W., and Meyskens, F. L., Jr. (2004) *Nat. Rev. Cancer* **4,** 781–792
19. Schipper, R. G., Penning, L. C., and Verhofstad, A. A. (2000) *Semin. Cancer Biol.* **10,** 55–68
20. Erwin, B. G., Ewton, D. Z., Florini, J. R., and Pegg, A. E. (1983) *Biochem. Biophys. Res. Commun.* **114,** 944–949
21. Kufe, D. W., Griffin, J., Mitchell, T., and Shafman, T. (1984) *Cancer Res.* **44,** 4281–4284
22. Nilsson, J. A., Keller, U. B., Baudino, T. A., Yang, C., Norton, S., Old, J. A., Nilsson, L. M., Neale, G., Kramer, D. L., Porter, C. W., and Cleveland, J. L. (2005) *Cancer Cell* **7,** 433–444
23. Mitchell, J. L., Judd, G. G., Bareyal-Leyser, A., and Ling, S. Y. (1994) *Biochem. J.* **299,** 19–22
24. Keren-Paz, A., Bercovich, Z., Porat, Z., Erez, O., Brener, O., and Kahana, C. (2006) *Oncogene* **25,** 5163–5172
25. Bartlett, M. S., Fishman, J. A., Queener, S. F., Durkin, M. M., Jay, M. A., and Smith, J. W. (1988) *J. Clin. Microbiol.* **26,** 1100–1102
26. Matsufuji, S., Miyazaki, Y., Kanamoto, R., Kameji, T., Murakami, Y., Baby, T. G., Fujita, K., Ohno, T., and Hayashi, S. (1990) *J. Biochem.* (*Tokyo*) **108,** 365–371
27. Matsufuji, S., Kanamoto, R., Murakami, Y., and Hayashi, S. (1990) *J. Biochem.* (*Tokyo*) **107,** 87–91
28. Murakami, Y., Ichiba, T., Matsufuji, S., and Hayashi, S. (1996) *J. Biol. Chem.* **271,** 3340–3342
29. Aouida, M., Leduc, A., Wang, H., and Ramotar, D. (2004) *Biochem. J.* **384,** 47–58
30. Wang, S. H., Zhang, C., Lasbury, M. E., Liao, C. P., Durant, P. J., Tschang, D., and Lee, C. H. (2008) *Microbes Infect.* **10,** 334–341
31. Kim, S. W., Mangold, U., Waghorne, C., Mobascher, A., Shantz, L., Banyard, J., and Zetter, B. R. (2006) *J. Cell Sci.* **119,** 2583–2591
32. Suzuki, O., Matsumoto, T., and Katsumata, Y. (1984) *Experientia* (*Basel*) **40,** 838–839
33. Schipper, R. G., Cuijpers, V. M., De Groot, L. H., Thio, M., and Verhofstad, A. A. (2004) *J. Histochem. Cytochem.* **52,** 1259–1266
34. Heiskala, M., Zhang, J., Hayashi, S., Holtta, E., and Andersson, L. C. (1999) *EMBO J.* **18,** 1214–1222
35. Cullis, P. M., Green, R. E., Merson-Davies, L., and Travis, N. (1999) *Chem. Biol.* **6,** 717–729
36. Soulet, D., Covassin, L., Kaouass, M., Charest-Gaudreault, R., Audette, M., and Poulin, R. (2002) *Biochem. J.* **367,** 347–357
37. Soulet, D., Gagnon, B., Rivest, S., Audette, M., and Poulin, R. (2004) *J. Biol. Chem.* **279,** 49355–49366
38. Hoet, P. H., and Nemery, B. (2000) *Am. J. Physiol.* **278,** L417–L433
39. Uemura, T., Kashiwagi, K., and Igarashi, K. (2007) *J. Biol. Chem.* **282,** 7733–7741
40. Roy, U. K., Rial, N. S., Kachel, K. L., and Gerner, E. W. (2008) *Mol. Carcinogr.* **47,** 538–553
41. Aziz, S. M., Yatin, M., Worthen, D. R., Lipke, D. W., and Crooks, P. A. (1998) *J. Pharm. Biomed. Anal.* **17,** 307–320
42. Merali, S. (1999) *J. Biol. Chem.* **274,** 21017–21022
43. Liu, G. Y., Liao, Y. F., Hsu, P. C., Chang, W. H., Hsieh, M. C., Lin, C. Y., Hour, T. C., Kao, M. C., Tsay, G. J., and Hung, H. C. (2006) *Apoptosis* **11,** 1773–1788
44. Cheng, Y., Chaturvedi, R., Asim, M., Bussiere, F. I., Scholz, A., Xu, H., Casero, R. A., Jr., and Wilson, K. T. (2005) *J. Biol. Chem.* **280,** 22492–22496
45. Chaturvedi, R., Asim, M., Lewis, N. D., Algood, H. M., Cover, T. L., Kim, P. Y., and Wilson, K. T. (2007) *Infect. Immun.* **75,** 4305–4315
46. Bussiere, F. I., Chaturvedi, R., Cheng, Y., Gobert, A. P., Asim, M., Blumberg, D. R., Xu, H., Kim, P. Y., Hacker, A., Casero, R. A., Jr., and Wilson, K. T. (2005) *J. Biol. Chem.* **280,** 2409–2412
47. Xu, H., Chaturvedi, R., Cheng, Y., Bussiere, F. I., Asim, M., Yao, M. D., Potosky, D., Meltzer, S. J., Rhee, J. G., Kim, S. S., Moss, S. F., Hacker, A., Wang, Y., Casero, R. A., Jr., and Wilson, K. T. (2004) *Cancer Res.* **64,** 8521–8525
48. Jung, M. H., Kim, S. C., Jeon, G. A., Kim, S. H., Kim, Y., Choi, K. S., Park, S. I., Joe, M. K., and Kimm, K. (2000) *Genomics* **69,** 281–286
49. Brown, G. D. (2006) *Nat. Rev. Immunol.* **6,** 33–43
50. Goodridge, H. S., Simmons, R. M., and Underhill, D. M. (2007) *J. Immunol.* **178,** 3107–3115
51. Chin, K., Merali, S., Saric, M., and Clarkson, A. B., Jr. (1996) *Antimicrob. Agents Chemother.* **40,** 2318–2320
52. Clarkson, A. B., Jr., Williams, D. E., and Rosenberg, C. (1988) *Antimicrob. Agents Chemother.* **32,** 1158–1163
53. Kaur, N., Delcros, J. G., Imran, J., Khaled, A., Chehtane, M., Tschammer, N., Martin, B., and Phanstiel, O. (2008) *J. Med. Chem.* **51,** 1393–1401